J. COMBIN. MATH. COMBIN. COMPUT. 127a (2025) 6539--6553

Journal of Combinatorial Mathematics and Combinatorial Computing
www.combinatorialpress.com/jcmcc

Semantic segmentation model for lane lines based on multi-scale attention mechanism

Rao Li[1,✉], Yaxiong Tao[1], Lingfeng Chen[2]

[1] *College of Communication Engineering, Chongqing Polytechnic University of Electronic Technology, Chongqing, 401331, China*

[2] *School of Information Engineering, Chongqing Vocational and Technical University of Mechatronics, Chongqing, 400000, China*

ABSTRACT
By improving the standard U-Net architecture, this paper proposes a novel semantic segmentation model, which incorporates multiple attention mechanisms to enhance the model's capacity to capture multi-scale features. Specifically, we introduce the Efficient Multi-Scale Attention Module with Cross-Spatial Learning (EMA), Spatial and Channel Squeeze and Excitation (SCSE), and Squeeze-and-Excitation (SE) mechanisms into the standard U-Net network. These modules assist the network in learning significant information from feature maps at multiple scales while suppressing interference from irrelevant background. Experimental results demonstrate that incorporating attention mechanisms effectively enhances the prediction accuracy of the standard U-Net network for lane line semantic segmentation. The new model outperforms the standard U-Net model on our custom dataset, with particularly significant improvements in lane detection accuracy in scenarios with certain interference.

Keywords: U-Net, Semantic segmentation, Lane detection, Attention mechanism

1. Introduction

With the development and maturity of the new generation of digital technologies such as artificial intelligence, Internet of Things, and 5G mobile communication, automatic driving technology is becoming more and more mature [1-2]. In the future, automatic driving still has a good development prospect and will develop in the direction of driverless. All major countries in the world have attached great importance to the development of automatic driving [3-4]. As China's comprehensive national power continues to improve, the rapid development of social and economic development, the people's living standards and quality of life has been continuously upgraded and improved, in order to meet the

✉ Corresponding author.
E-mail address: lirao@cqcet.edu.cn (R. Li).
Received 05 March 2024; Revised 25 May 2024; Accepted 05 December 2024; Published Online 15 April 2025.
DOI: 10.61091/jcmcc127a-362

demand for high-quality travel, new modes of transportation and innovative transportation services continue to emerge, but traffic congestion and traffic accidents are still the main problems and challenges faced by the traffic travel [5-8]. Traffic accidents not only bring significant economic losses, but also cause serious consequences such as casualties [9]. In order to solve the related problems, countries have introduced relevant policies and systems to improve transportation services, and the industry and academia have also focused on emerging technologies to innovate transportation technologies, and various intelligent technologies have been popularized and applied in vehicle-assisted driving systems [10-13]. In order to reduce traffic accidents, alleviate road congestion, and improve people's quality of life, academia and industry have conducted in-depth research on advanced assisted driving systems and autonomous driving systems [14-16].

Lane lines, as important traffic signs, carry intuitive road information, which is important for ensuring the safety and stability of autonomous driving systems and assisting drivers to make correct decisions [17-18]. Lane line detection, as one of the core cornerstones in the automatic driving technology system, plays a pivotal role in the environment perception algorithm [19-20]. Its core function lies in accurately extracting road surface feature information to provide decision support for the self-driving vehicle, thus ensuring that the vehicle can drive safely, stably and reliably [21-22]. In advanced assisted driving systems, lane line detection technology plays an indispensable support role for the completion of basic tasks such as direction keeping, lane changing, offset warning, forward collision warning, intelligent cruise control and emergency braking [23-25]. Together, these functions guarantee the safety and comfort of driving and promote the continuous progress of intelligent driving technology [26].

Literature [27] describes the underlying logic and commercial application scenarios of lane departure systems, and comparatively analyzes the performance of traditional image processing and semantic segmentation in lane departure systems. Literature [28] conceptualized a lane segmentation monitoring method with semantic segmentation as the core logic, and evaluated and tested it in conjunction with cityscape database to confirm the feasibility of the proposed Lane-DeepLab. Literature [29] based on a computer vision algorithm pipeline that enables lane line detection algorithms to enhance each other, and based on this, a reliable lane line detection and tracking technique is envisioned, and in evaluation tests, the proposed lane line detection and tracking technique is confirmed to be fully adapted for intelligent assisted driving. Literature [30] conceived a new safe lane change trajectory model and anti-collision control strategy, and tested them in a physical simulation platform, which provides an important reference for the research of automated intelligent driving. Literature [31] envisioned an advanced road detection and tracking scheme, in which the focus is on the convenient and accurate identification and prediction of lanes, and verified the effectiveness of the scheme in lane detection as well as road tracking through real tests. Literature [32] introduces Lanelet2, an open source map framework developed in C++ to accurately match intelligent automated driving, and provides an advanced demonstration of the open source map framework Lanelet2 structure as well as automated driving applications.

To address these limitations, this paper proposes an enhanced version of the U-Net model to improve its ability to extract features across multiple scales by introducing EMA, SCSE, and SE modules. These attention mechanisms allow the network to focus on critical regions of lane lines, thereby effectively enhancing detection accuracy. The main contributions of this paper are as follows.

1) A novel U-Net architecture that integrates EMA, SCSE, and SE modules is proposed to improve the model's ability to learn multi-scale features.

2) The effectiveness of the proposed method is validated on a custom dataset, taking into account interference scenarios such as rainy conditions, strong lighting, and road wear. Experimental results show that the new model achieves superior performance across diverse conditions.

3) The impact of each attention module on the model's performance is analyzed in detail through experiments, offering valuable insights for future research on semantic segmentation problems.

2. Network Architecture

U-Net is a convolutional neural network architecture originally designed for medical image segmentation, where it demonstrated high performance. The U-Net architecture consists of an encoder that extracts image features and a decoder that reconstructs these features into a segmentation mask of the same size as the input. A prominent feature of U-Net is the implementation of Skip Connections, which directly connects the feature maps of each layer in the encoder to the corresponding layer in the decoder. This approach provides the decoder with access to high-resolution features from the early stages of the encoder, which is crucial for recovering details and boundaries.

In recent years, attention mechanisms have received significant attention in computer vision tasks. The attention mechanism allows models to focus on which parts of the input are most influential to the output. Additionally, the attention mechanism captures long-range dependencies, enabling the model to directly reference the entire encoder's output during decoding, thereby improving the processing of long sequences.

In EMA, in addition to recalibrating the channel weights in each parallel branch by encoding global information, the output features of both parallel branches are aggregated through cross-dimensional interaction to capture pixel-level pairing relationships. This parallel subnet design effectively facilitates the capture of inter-dimensional interactions and the establishment of inter-dimensional dependencies. EMA focuses on preserving information in each channel while minimizing computational overhead by reshaping certain channels into batch dimensions and grouping channel dimensions into multiple sub-features, thereby ensuring that spatial semantic features are evenly distributed across each feature group. SCSE combines spatial and channel attention mechanisms. Spatial attention mechanisms emphasize specific regions in the image, while channel attention mechanisms prioritize the most relevant channels in the feature map. The SCSE module enhances feature representation by computing the weight of each spatial position and the importance of each channel, enabling the model to focus more effectively on the target object. By adaptively reweighting each feature map. the SE module enables the network to dynamically adjust attention resources to focus on the most useful information. This mechanism first compresses global information, then generates weight coefficients for each channel through the excitation process, and finally applies these weights to the original feature map.

According to the characteristics of the lane dataset, we implement specific improvements to the standard U-Net network structure. Specifically, EMA modules are integrated into each skip connection, meaning that data is fed into the EMA module before each downsampling and then fused with the upsampling data. This process effectively mitigates data loss caused by downsampling and enhances feature extraction. The core concept of EMA's enhanced feature extraction lies in feature grouping and parallel subnetworks. For any given input feature map $X \in \mathbf{R}^{C \times H \times W}$, EMA divides it into G sub-features along the channel dimension to learn diverse semantic information.

SCSE modules are incorporated into several convolutional layers of U-Net encoders and decoders to enhance feature representation. The SCSE module integrates both spatial and channel attention mechanisms. In the channel attention mechanism, the input feature map, denoted as $U = [u_1, u_2, ..., u_c]$, is composed of multiple channels, where $u_i \in \mathbf{R}^{H \times W}$ refers to an individual channel. The channel attention is obtained by applying spatial squeezing through a global average pooling layer, generating a vector $z \in \mathbf{R}^{C}$, where z_k denotes the global average of the K-th channel.

$$z_k = \frac{1}{H \times W} \sum_{i=0}^{H-1} \sum_{j=0}^{W-1} u_k(i, j) \tag{1}$$

Subsequently, this vector undergoes transformation via two fully connected layers and is processed through the ReLU activation function.

$$\hat{z} = \sigma(W_1 \delta(W_2 z)) \tag{2}$$

Where, $W_1 \in \mathbf{R}^{C\times\frac{C}{2}}$, $W_2 \in \mathbf{R}^{\frac{C}{2}\times C}$, δ is the ReLU activation function. Then, $\hat{z}$ is normalized to the interval [0,1] by the sigmoid activation function to recalibrate the input feature map.

$$\hat{U}_C = [\sigma(\hat{z}_1)u_1, \sigma(\hat{z}_2)u_2, ..., \sigma(\hat{z}_c)u_c] \tag{3}$$

In the spatial attention mechanism, the input feature map is conceptualized as a series of positions represented by $U = [u_{1,1}, u_{1,2}, \ldots, u_{i,j}, \ldots, u_{H,W}]$, where $u_{i,j} \in \mathbf{R}^{1\times1\times C}$ denotes the feature vector at position (i, j). The spatial attention mechanism executes spatial compression of the input feature map through the convolution operation $q = W_{sq} * U$, with $W_{sq} \in \mathbf{R}^{1\times1\times C\times1}$ generating a projection tensor $q \in \mathbf{R}^{H\times W}$. This projection is subsequently normalized to the interval [0, 1] using the sigmoid function, which serves to calibrate the input feature map.

$$U_s = [\sigma(q_{1,1})u_{1,1}, ..., \sigma(q_{i,j})u_{i,j}, ..., \sigma(q_{H,W})u_{H,W}] \tag{4}$$

Following the SCSE module, the SE module is introduced to enhance channel-level features further. The SE attention mechanism autonomously learns the significance of various channels by compressing and activating the channel dimensions. This mechanism is mathematically represented by Eq. (5):

$$M_{se}(F) = \sigma(MLP(AvgPool(F))) = MLP(F_c) = \sigma(W_1(W_0(F_c))) \tag{5}$$

Where F represents the input feature map, W_0 and W_1 are the weight matrices of the two fully connected layers, F_c is the channel dimension feature vector after average pooling, and σ represents the sigmoid activation function. After passing through the SCSE module, the output feature chart is Eq. (6):

$$F_{out} = M_{se}(F) \otimes F \tag{6}$$

Figure 1 illustrates the comprehensive architecture of the network, wherein the EMA, SCSE, and SE modules enhance feature extraction across multiple scales. Notably, these modules do not alter the dimensions of the image.

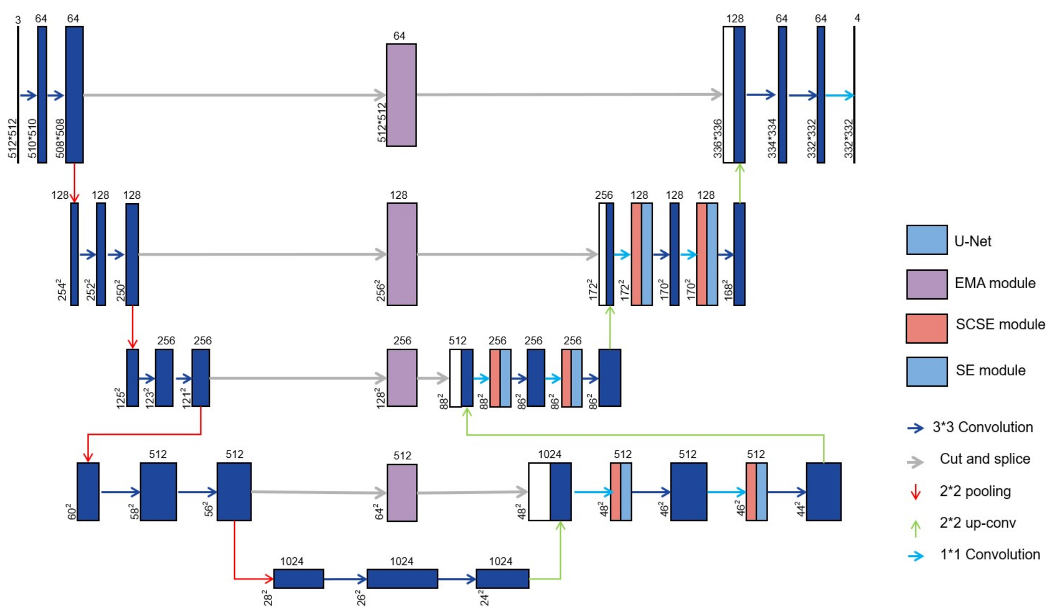

Fig. 1. Network Architectures

3. Experiment

Firstly, the evaluation was conducted using the standard U-Net architecture, with metrics such as mIoU, MPA, Mean Precision, and Mean Recall computed on the test dataset. Subsequently, EMA, SCSE, and SE were individually integrated into the U-Net framework for testing purposes to assess each module's impact on the model's overall performance. Additionally, we examined how each attention module responded to various interference scenarios. Finally, EMA, SCSE, and SE modules were incorporated into the standard U-Net network following the structure illustrated in Figure 1 to further investigate potential enhancements in relevant performance indicators.

3.1. Dataset

A custom dataset was used in the experiment, consisting of a total of 15,000 images of lane lines across various traffic scenarios. Specifically, the dataset includes annotations for solid lane lines, dotted lane lines, and Zebra crossing. The dataset is highly diverse, featuring scenarios with varying weather conditions, lighting, and road types. Images and corresponding labels in the dataset are provided at a resolution of 1920*1080 pixels. Figure 2 presents some sample images and labels from the dataset.

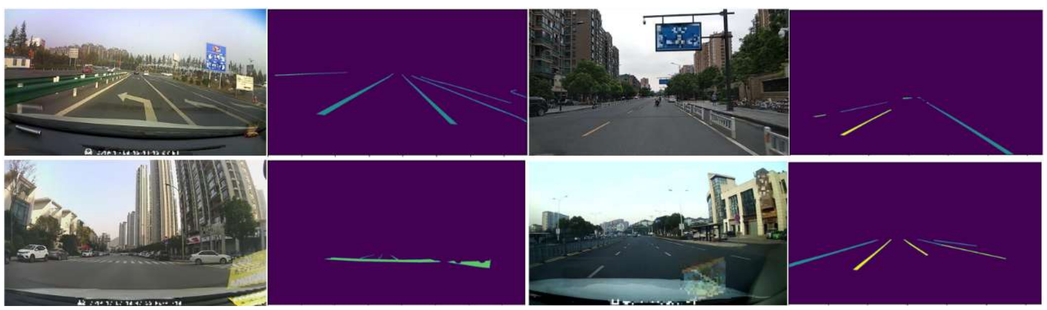

Fig. 2. A portion of the dataset consisting of images and corresponding label

Prior to training, the dataset underwent preprocessing, involving random rotation, horizontal flipping, and brightness adjustment. Additionally, label data image values were standardized to enhance the effectiveness of model training.

The dataset was randomly divided into a training set (80%), a validation set (10%), and a test set (10%). In terms of evaluation metrics, Mean Intersection over Union (mIoU) and Mean Pixel Accuracy (MPA) served to assess the overall performance of the model. Specifically, IoU and MPA are core evaluation metrics in semantic segmentation tasks, with IoU typically used to measure the degree of overlap between two areas (usually bounding boxes or segmentation masks). MPA is a metric for image segmentation tasks, measuring the proportion of predicted labels that agree with real labels per pixel. For an image segmentation task with multiple categories, MPA calculates the average pixel accuracy for each category.

Among the evaluation indicators in Table 1, TP_i is the number of correctly predicted True Positives in category i. FP_i is the number of False Positives incorrectly predicted for the i class. FN_i is the number of pixels in the i class that are incorrectly predicted as other classes (False Negatives). IoU_i tinna Indicates the IoU of category i. N_{total} represents the total number of pixels in the image. N represents the total number of categories. $Precision_i$ represents the accuracy of category i. $Recall_i$ represents the recall rate for Category i.

Table 1. Evaluation Metrics

Metrics	Full name	Formula

IoU	Intersection over Union	$\text{IoU}_i=\frac{TP_i}{TP_i+FP_i+FN_i}$
mIoU	Mean Intersection over Union	$m\text{IoU}=\frac{1}{N}\sum_{i=1}^{N}\text{IoU}_i$
MPA	Mean Pixel Accuracy	$MPA=\frac{1}{N_{total}}\sum_{i=1}^{N}TP_i$
Precision	Precision	$Precision_i=\frac{TP_i}{TP_i+FP_i}$
Recall	Recall	$Recall_i=\frac{TP_i}{TP_i+FN_i}$

Unlike classification problems, in semantic segmentation, it is typically necessary to compute the average Precision and Recall of all categories, namely Mean Precision and Mean Recall.

$$Mean\ Precision=\frac{1}{N}\sum_{i=1}^{N}Precision_i \tag{7}$$

$$Mean\ Recall=\frac{1}{N}\sum_{i=1}^{N}Recall_i \tag{8}$$

3.2. Model training

To prevent the decentralization value of the backbone network from becoming too scattered and random, VGG16 was employed as the backbone network pre-training weight during the model training process. The model utilized the VGG16 network as the encoder in U-Net, with the model weights pre-trained on the Pascal VOC dataset. VGG16 is a widely adopted convolutional neural network (CNN) architecture. Due to its simple design and high performance, it has been extensively applied in various computer vision tasks, particularly image classification. This pre-trained weight file can initialize another U-Net model, facilitating fine-tuning on a new task without the need to train from scratch, significantly saving time and computational resources. These pre-trained weights exhibit a degree of generalizability across different datasets and can significantly enhance the feature extraction capabilities of the model.

Model training was conducted using the Ubuntu 20.04 operating system and PyTorch 2.3.0 as the deep learning framework. Hardware configuration was as follows. CPU: Intel(R) Xeon(R) W5-2455X, Graphics Card: NVIDIA RTX A5000, 24GB, CUDA Version: 11.7. Key hyperparameters established for training are presented in Table 2.

Table 2. Hyperparameter

Hyperparameter	Values	Remarks
num_classes	4	Categories
backbone	vgg	Pre-initialized Weights
epoch	100	Quantity of iterations
batch_size	4	Batch size
learning_rate	le-4	Learning rate
optimizer	Adam	Optimizer
sync_bin	False	Whether to use mixed precision

3.3. Experimental results

To verify the role and influence of each attention module, an ablation study was conducted. Initially, the basic U-Net architecture was used for testing. The test data were evaluated using the optimally trained model, and the metrics mIoU, MPA, Mean Precision, and Mean Recall were calculated for the test set.

As shown in Figure 3, according to the test set results, the mIoU index was 68.68%, while the MPA index reached 77.04%, with no indication of overfitting. To verify the contribution of each attention mechanism in the architecture, we incorporated each attention module into the U-Net framework during experimentation to observe their respective roles and impact. Initially, the EMA attention mechanism was integrated into the skip connection component of U-Net to enhance feature extraction and mitigate information loss resulting from downsampling.

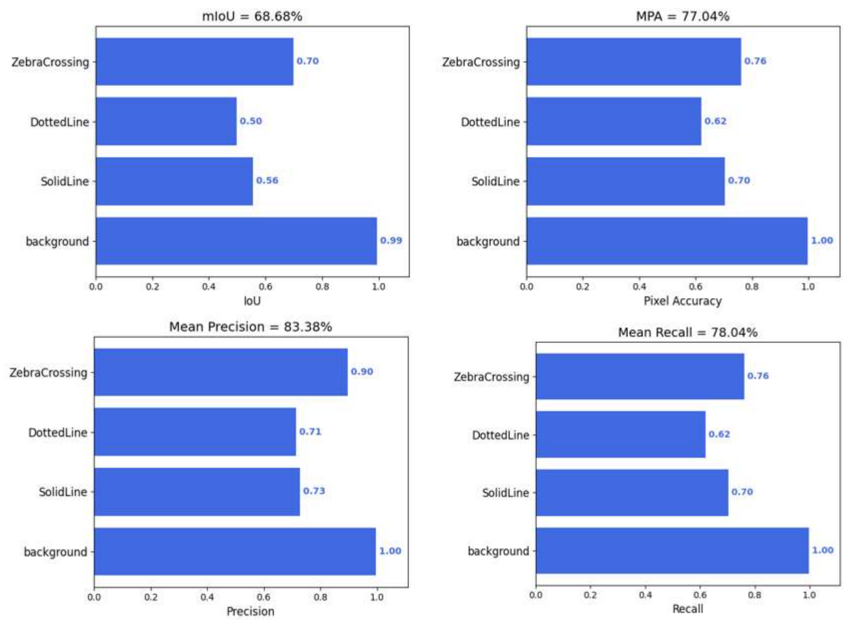

Fig. 3. The mIoU, MPA, Mean Precision, and Mean Recall metrics on the test set utilizing the standard U-Net architecture

As shown in Figure 4, based on the experimental results, the incorporation of the EMA module into the U-Net architecture led to a 2.37% increase in the mIoU index, a 1.5% improvement in the MPA index, a 1.38% rise in Mean Precision, and a 1% decrease in the Mean Recall index. Testing the data in the test set, as shown in Figure 5, demonstrates that incorporating the EMA attention mechanism enables the model to focus more on lane line-related content, thereby reducing the number of incorrectly predicted pixels.

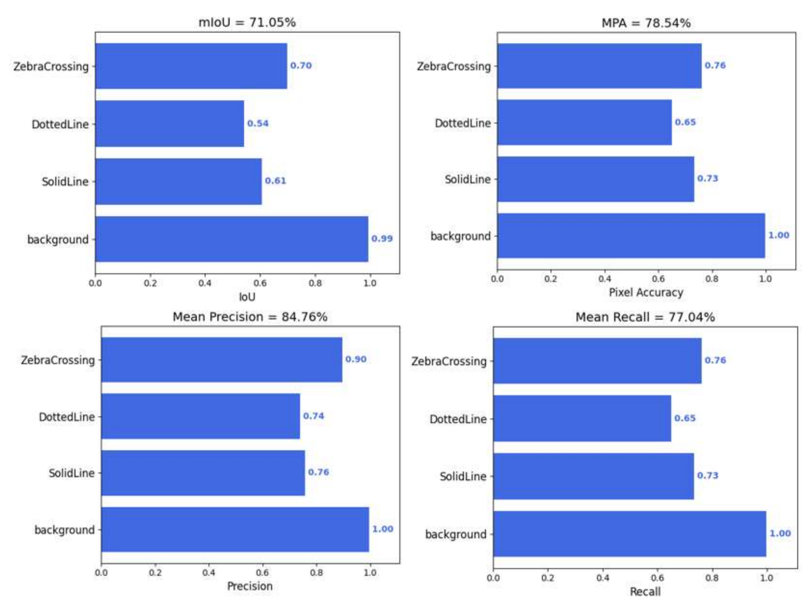

Fig. 4. The mIoU, MPA, Mean Precision, and Mean Recall metrics of the U-Net network on the test set were evaluated after incorporating the EMA attention mechanism

Fig. 5. The Standard U-Net architecture and the mIoU curve on the validation set following the incorporation of the EMA mechanism

SCSE combines spatial and channel attention mechanisms, facilitating the extraction of finer image features. The channel attention mechanism enables the network to learn the dependencies among different feature maps and reassign the importance of each feature accordingly. This approach proves useful for extracting global information about lane lines, as they may be more visible in certain regions, with channel attention able to emphasize such regions. The spatial attention mechanism focuses on the distribution of features across spatial dimensions and generates a weight map to emphasize critical pixels or regions. For lane detection, this aids in capturing the precise shape and position of lane lines and helps maintain high detection accuracy even in the presence of complex backgrounds or occlusions. By combining these two mechanisms, SCSE enhances the network's ability to more accurately identify and segment lane lines, particularly in complex scenarios. For instance, on highways or urban roads, a variety of interfering factors, such as vehicles, pedestrians, trees, and signs, may be present. SCSE enables the model to disregard these factors and focus on lane lines, thus improving segmentation accuracy. The experiment assesses the impact of the SCSE module on the model's overall performance by incorporating it individually before each skip connection. Upon integrating the SCSE attention mechanism into the U-Net framework, the metrics mIoU, MPA, Mean Precision, and Mean Recall are presented in Figure 6.

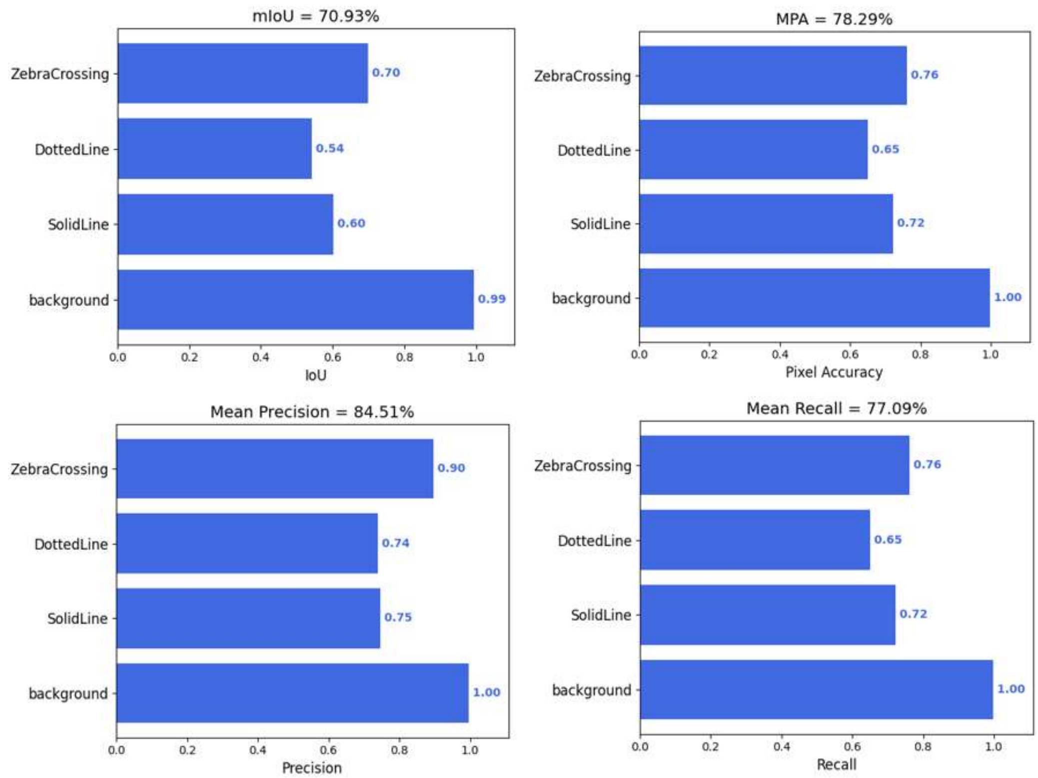

Fig. 6. The mIoU, MPA, Mean Precision, and Mean Recall metrics of the U-Net network on the test set were evaluated after incorporating the SCSE attention mechanism

The experimental results indicate that the incorporation of the SCSE attention mechanism can mitigate interference to a certain degree and enhance feature extraction efficacy. As illustrated in the upper section of Figure 7, the standard U-Net architecture predicts numerous curb positions as solid lane markings; however, when the SCSE attention mechanism is integrated, there is a significant reduction in mislabeled pixels. In the lower portion of Figure 7, it is evident that the standard U-Net architecture lacks precision in detail processing—such as incorrectly designating distant areas with poor visibility as sidewalks—but with the addition of the SCSE attention mechanism, these details are rendered more distinctly, effectively decreasing the number of misclassified pixels.

Fig. 7. In comparison to the prediction outcomes of the standard U-Net network enhanced with the SCSE attention module, the inference results of the standard U-Net network are presented on the left, while those incorporating the SCSE attention module are illustrated in the image on the right

The SE attention mechanism acquires global information from each feature map via Global Average Pooling and produces weights for each channel through Fully Connected Layers. These weights are subsequently employed to reweight the feature map of each channel, enabling the network to concentrate more on the significant features. In the task of semantic segmentation of lane lines, the SE mechanism can assist the model in capturing the features of lane lines more effectively. Given that lane lines might occupy a small portion of the image and be disturbed by background noise, the SE mechanism can facilitate the model to spotlight these crucial features and enhance the accuracy of segmentation. Additionally, the SE module has a straightforward structure and can be effortlessly integrated into the neural network structure. Considering that the module is situated in the upper sampling part of the entire structure, its primary function is to reinforce feature selection and reduce the quantity of model parameters. Upon integrating the SCSE attention mechanism into the U-Net framework, the metrics mIoU, MPA, Mean Precision, and Mean Recall are presented in Figure 8.

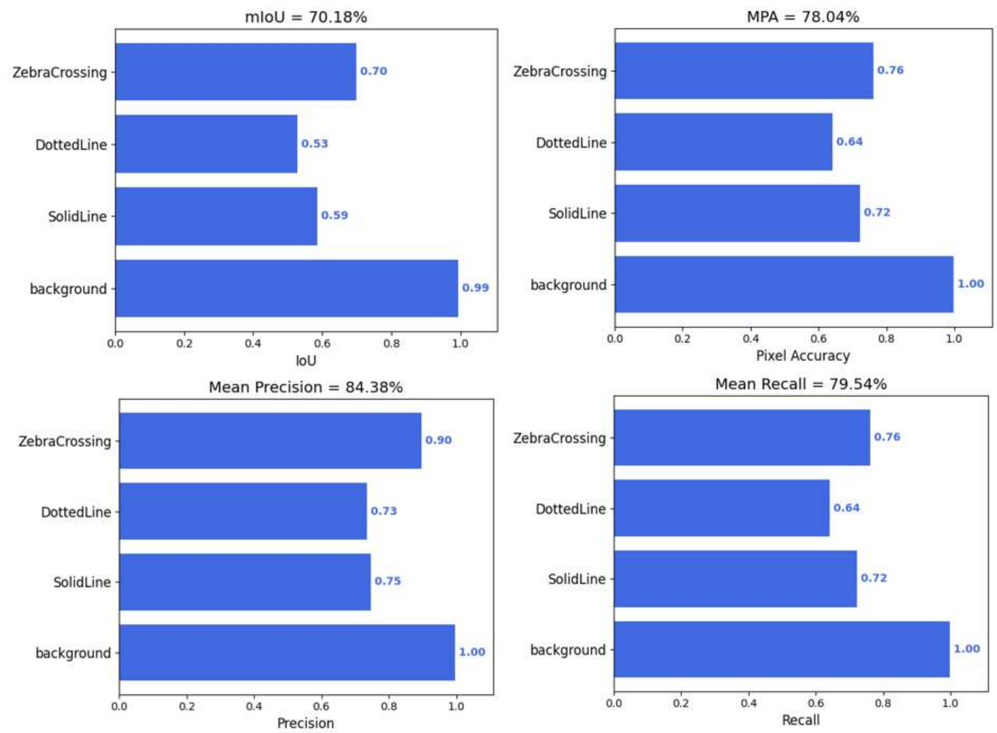

Fig. 8. The mIoU, MPA, Mean Precision, and Mean Recall metrics of the U-Net network on the test set were evaluated after incorporating the SE attention mechanism

From the test results, upon the sole addition of the SE attention mechanism, core indicators such as mIoU and MPA have been enhanced to a certain extent. Regarding the specific details, the SE attention mechanism demonstrates superior error correction capabilities in aspects like unclear lane lines and misrecognition. In Figure 9, the U-Net network fails to effectively identify the unclear lane lines resulting from wear and tear, whereas the new model incorporating the SE attention mechanism can effectively do so. In Figure 9, U-Net misidentifies the grid area dedicated to fire protection as a sidewalk, and the inclusion of SE attention can effectively prevent this occurrence.

Fig. 9. The In comparison to the prediction outcomes of the standard U-Net network enhanced with the SE attention module, the inference results of the standard U-Net network are presented on the left, while those incorporating the SE attention module are illustrated in the image on the right

Based on the analysis of prior experimental results, the standard U-Net architecture can enhance model performance at various levels by incorporating MEA, SCSE, and SE modules individually. As shown in Figure 10 to Figure 13 and Table 3, the MEA module contributes to improved convergence stability, while both SCSE and SE modules increase the model's adaptability to diverse interference scenarios and significantly enhance the mIoU index. These three modules have now been integrated into the network structure illustrated in Figure 1 for comprehensive testing and analysis.

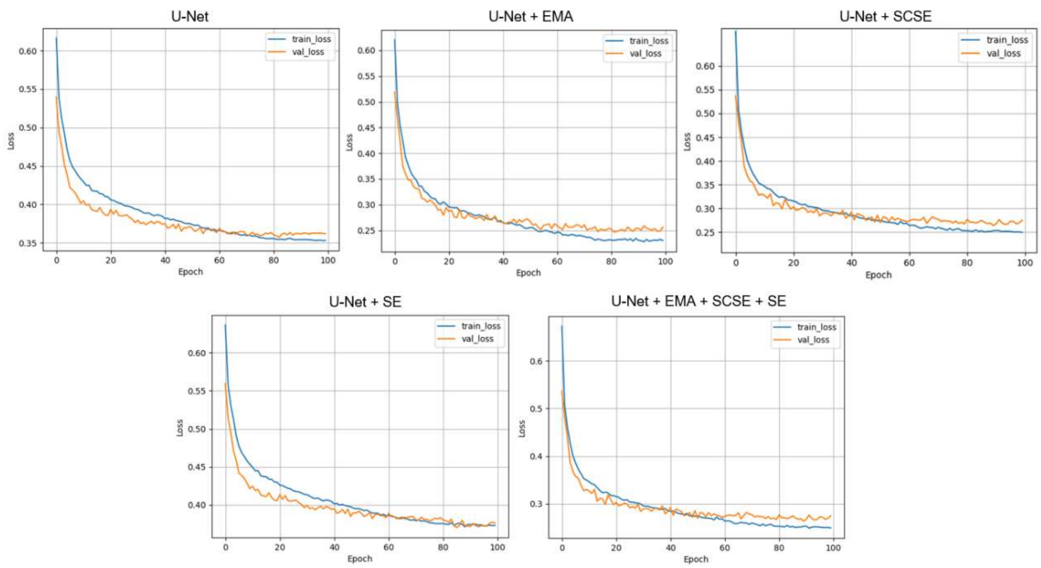

Fig. 10. Variations in the U-Net loss function during the training process with the incorporation of EMA, SCSE, and SE modules

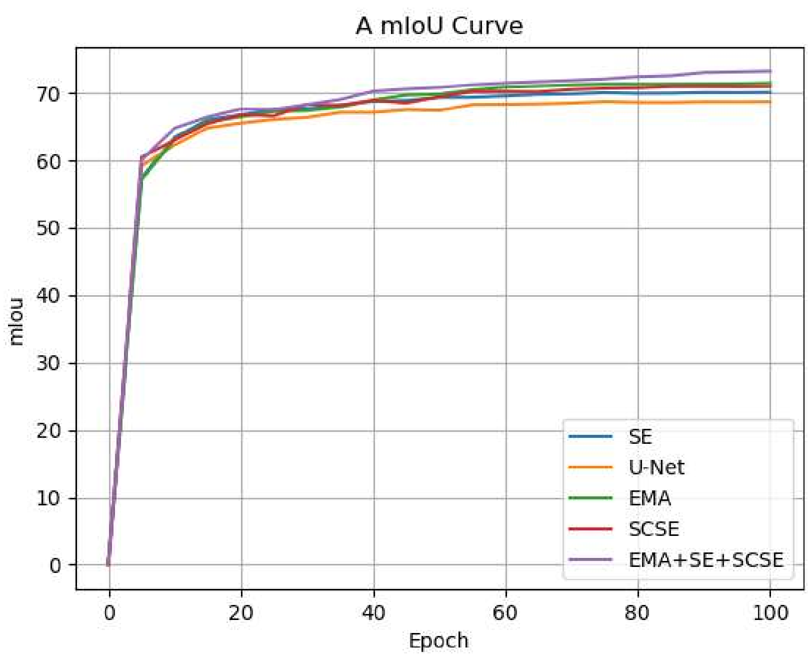

Fig. 11. The variation in mIoU of the U-Net network, enhanced with EMA, SCSE, and SE modules, on the validation set

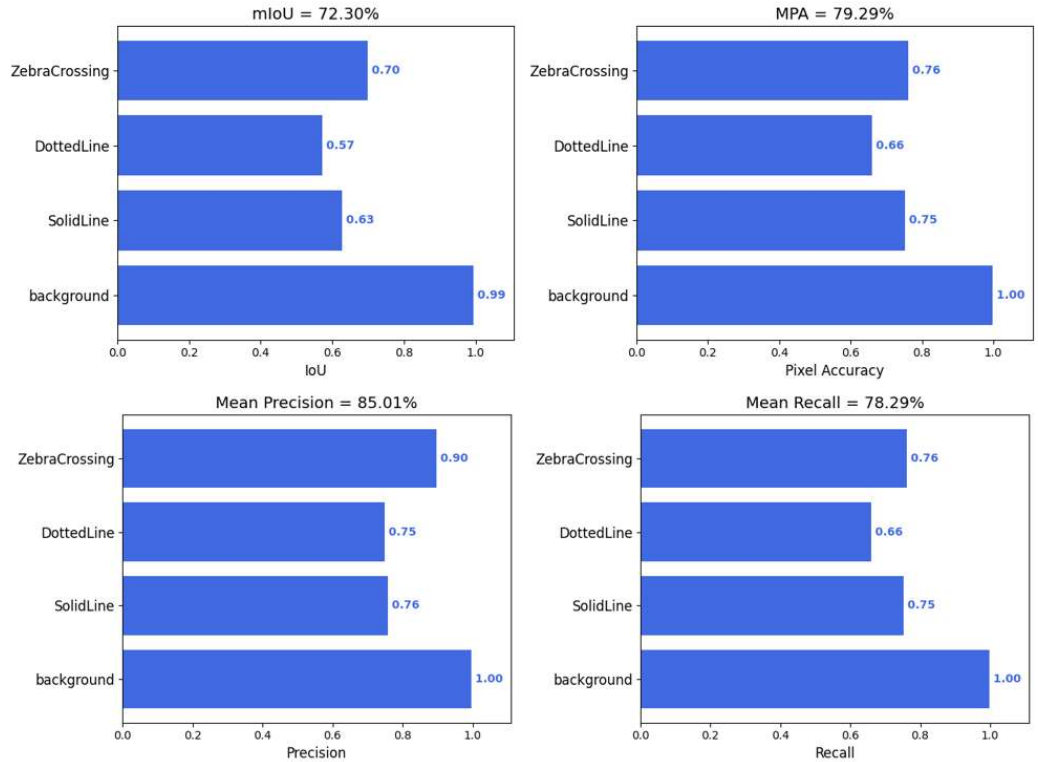

Fig. 12. The mIoU, MPA, Mean Precision, and Mean Recall metrics on the test set were evaluated after incorporating EMA, SCSE, and SE attention mechanisms into the standard U-Net architecture

Table 3. Results of mIoU, MPA, Mean Precision, and Mean Recall Metrics across Different Network Architectures

Network Architectures	mIoU	MPA	Mean Precision	Mean Recall
U-Net	68.68%	77.04%	83.38%	78.04%
U-Net + EMA	71.05%	78.54%	84.76%	77.04%
U-Net + SCSE	70.93%	78.29%	84.51%	77.09%
U-Net + SE	70.18%	78.04%	84.38%	79.54%
U-Net+EMA+SCSE+SE	72.30%	79.29%	85.01%	78.29%

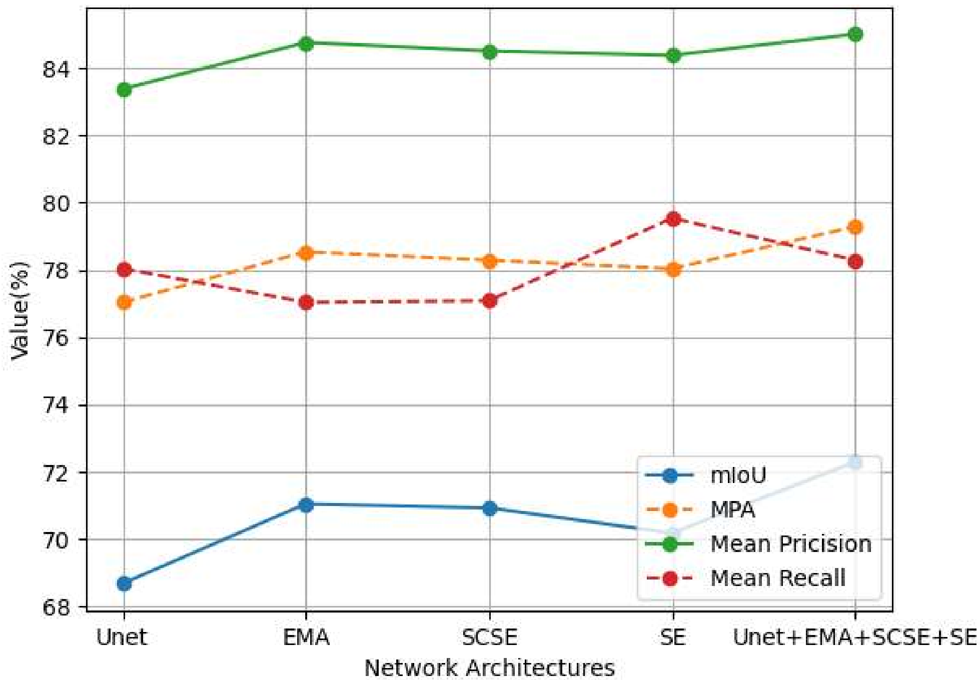

Fig. 13. Comparison of mIoU, MPA, Mean Precision, and Mean Recall Metrics across Different Network Architectures

4. Conclusion

Based on the U-Net network, this paper presents a novel semantic segmentation model for lane lines by incorporating an attention mechanism. This paper examines the effects of EMA, SCSE, and SE attention modules on U-Net networks. Experimental results indicate that EMA not only enhances the model's performance metrics but also efficiently handles interference. SCSE is more effective in handling specific interference scenarios, whereas SE is better at addressing blurred scenes caused by lane wear. Additionally, the combination of multiple attention mechanisms led to significant improvements in core metrics such as mIoU and MPA. Compared to the standard U-Net network, mIoU increased by 3.62%, MPA by 2.25%, Mean Precision by 1.63%, and Mean Recall by 0.25%. Experimental results demonstrate that attention mechanisms can significantly enhance the overall performance of semantic segmentation models, while also improving the accuracy and robustness of the U-Net network for lane line segmentation.

Funding

This work was supported by the Science and Technology Research Program of the Chongqing Education Commission (No. KJQN202403106).

References

[1] Li, X., Li, J., Hu, X., & Yang, J. (2019). Line-cnn: End-to-end traffic line detection with line proposal unit. IEEE Transactions on Intelligent Transportation Systems, 21(1), 248-258.

[2] Cesari, G., Schildbach, G., Carvalho, A., & Borrelli, F. (2017). Scenario model predictive control for lane change assistance and autonomous driving on highways. IEEE Intelligent transportation systems magazine, 9(3), 23-35.

[3] Zhang, T., Wang, L., Li, H., Xiao, Y., Liang, S., Liu, A., ... & Tao, D. (2024, October). Lanevil: Benchmarking the robustness of lane detection to environmental illusions. In Proceedings of the 32nd ACM International Conference on Multimedia (pp. 5403-5412).

[4] Ding, Y., Zhuang, W., Wang, L., Liu, J., Guvenc, L., & Li, Z. (2021). Safe and optimal lane-change path planning for automated driving. Proceedings of the Institution of Mechanical Engineers, Part D: Journal of Automobile Engineering, 235(4), 1070-1083.

[5] Yang, D., Zheng, S., Wen, C., Jin, P. J., & Ran, B. (2018). A dynamic lane-changing trajectory planning model for automated vehicles. Transportation Research Part C: Emerging Technologies, 95, 228-247.

[6] Narote, S. P., Bhujbal, P. N., Narote, A. S., & Dhane, D. M. (2018). A review of recent advances in lane detection and departure warning system. Pattern Recognition, 73, 216-234.

[7] Merat, N., Seppelt, B., Louw, T., Engström, J., Lee, J. D., Johansson, E., ... & Keinath, A. (2019). The "Out-of-the-Loop" concept in automated driving: proposed definition, measures and implications. Cognition, Technology & Work, 21, 87-98.

[8] Kukkala, V. K., Tunnell, J., Pasricha, S., & Bradley, T. (2018). Advanced driver-assistance systems: A path toward autonomous vehicles. IEEE Consumer Electronics Magazine, 7(5), 18-25.

[9] Wu, J., Xu, H., & Zhao, J. (2018). Automatic lane identification using the roadside LiDAR sensors. IEEE Intelligent Transportation Systems Magazine, 12(1), 25-34.

[10] Xia, Q., Duan, J., Gao, F., Hu, Q., & He, Y. (2018). Test scenario design for intelligent driving system ensuring coverage and effectiveness. International Journal of Automotive Technology, 19, 751-758.

[11] Feng, Z., Guo, S., Tan, X., Xu, K., Wang, M., & Ma, L. (2022). Rethinking efficient lane detection via curve modeling. In Proceedings of the IEEE/CVF Conference on Computer Vision and Pattern Recognition (pp. 17062-17070).

[12] Kortli, Y., Gabsi, S., Voon, L. F. L. Y., Jridi, M., Merzougui, M., & Atri, M. (2022). Deep embedded hybrid CNN–LSTM network for lane detection on NVIDIA Jetson Xavier NX. Knowledge-based systems, 240, 107941.

[13] Duan, J., Gao, F., & He, Y. (2020). Test scenario generation and optimization technology for intelligent driving systems. IEEE Intelligent Transportation Systems Magazine, 14(1), 115-127.

[14] Zheng, Y., & Hansen, J. H. (2017). Lane-change detection from steering signal using spectral segmentation and learning-based classification. IEEE Transactions on Intelligent Vehicles, 2(1), 14-24.

[15] Cao, J., Song, C., Song, S., Xiao, F., & Peng, S. (2019). Lane detection algorithm for intelligent vehicles in complex road conditions and dynamic environments. Sensors, 19(14), 3166.

[16] Wang, P., Gao, S., Li, L., Sun, B., & Cheng, S. (2019). Obstacle avoidance path planning design for autonomous driving vehicles based on an improved artificial potential field algorithm. Energies, 12(12), 2342.

[17] Sentouh, C., Nguyen, A. T., Benloucif, M. A., & Popieul, J. C. (2018). Driver-automation cooperation oriented approach for shared control of lane keeping assist systems. IEEE Transactions on Control Systems Technology, 27(5), 1962-1978.

[18] Gao, F., Duan, J., He, Y., & Wang, Z. (2019). A test scenario automatic generation strategy for intelligent

driving systems. Mathematical Problems in Engineering, 2019(1), 3737486.

[19] Zhang, X., & Zhu, X. (2019). Autonomous path tracking control of intelligent electric vehicles based on lane detection and optimal preview method. Expert Systems with Applications, 121, 38-48.

[20] Althoff, M., Urban, S., & Koschi, M. (2018, July). Automatic conversion of road networks from opendrive to lanelets. In 2018 IEEE International Conference on Service Operations and Logistics, and Informatics (SOLI) (pp. 157-162). IEEE.

[21] Lin, D., Li, L., & Jabari, S. E. (2019). Pay to change lanes: A cooperative lane-changing strategy for connected/automated driving. Transportation Research Part C: Emerging Technologies, 105, 550-564.

[22] Xing, Y., Lv, C., Chen, L., Wang, H., Wang, H., Cao, D., ... & Wang, F. Y. (2018). Advances in vision-based lane detection: Algorithms, integration, assessment, and perspectives on ACP-based parallel vision. IEEE/CAA Journal of Automatica Sinica, 5(3), 645-661.

[23] Liang, D., Guo, Y. C., Zhang, S. K., Mu, T. J., & Huang, X. (2020). Lane detection: A survey with new results. Journal of Computer Science and Technology, 35, 493-505.

[24] Pannen, D., Liebner, M., Hempel, W., & Burgard, W. (2020, May). How to keep HD maps for automated driving up to date. In 2020 IEEE International Conference on Robotics and Automation (ICRA) (pp. 2288-2294). IEEE.

[25] Suh, J., Chae, H., & Yi, K. (2018). Stochastic model-predictive control for lane change decision of automated driving vehicles. IEEE Transactions on Vehicular Technology, 67(6), 4771-4782.

[26] Jung, J., & Bae, S. H. (2018). Real-time road lane detection in urban areas using LiDAR data. Electronics, 7(11), 276.

[27] Chen, W., Wang, W., Wang, K., Li, Z., Li, H., & Liu, S. (2020). Lane departure warning systems and lane line detection methods based on image processing and semantic segmentation: A review. Journal of traffic and transportation engineering (English edition), 7(6), 748-774.

[28] Li, J., Jiang, F., Yang, J., Kong, B., Gogate, M., Dashtipour, K., & Hussain, A. (2021). Lane-DeepLab: Lane semantic segmentation in automatic driving scenarios for high-definition maps. Neurocomputing, 465, 15-25.

[29] Farag, W., & Saleh, Z. (2018, November). Road lane-lines detection in real-time for advanced driving assistance systems. In 2018 International Conference on Innovation and Intelligence for Informatics, Computing, and Technologies (3ICT) (pp. 1-8). IEEE.

[30] Peng, T., Su, L., Zhang, R., Guan, Z., Zhao, H., Qiu, Z., ... & Xu, H. (2020). A new safe lane-change trajectory model and collision avoidance control method for automatic driving vehicles. Expert Systems with Applications, 141, 112953.

[31] Farag, W. (2020). A comprehensive real-time road-lanes tracking technique for autonomous driving. International Journal of Computing and Digital Systems, 9(03).

[32] Poggenhans, F., Pauls, J. H., Janosovits, J., Orf, S., Naumann, M., Kuhnt, F., & Mayr, M. (2018, November). Lanelet2: A high-definition map framework for the future of automated driving. In 2018 21st international conference on intelligent transportation systems (ITSC) (pp. 1672-1679). IEEE.